Bio-Design and Manufacturing (2024) 7:611–623
https://doi.org/10.1007/s42242-024-00298-y

RESEARCH ARTICLE

Rapid fabrication of modular 3D paper-based microfluidic chips using projection-based 3D printing

Mingjun Xie[1,2,3,4,5] · Zexin Fu[1] · Chunfei Lu[2,3,4,5] · Sufan Wu[1] · Lei Pan[1] · Yong He[2,3,4,5] · Yi Sun[1] · Ji Wang[1]

Received: 6 July 2023 / Accepted: 15 May 2024 / Published online: 17 August 2024

Abstract

Paper-based microchips have different advantages, such as better biocompatibility, simple production, and easy handling, making them promising candidates for clinical diagnosis and other fields. This study describes a method developed to fabricate modular three-dimensional (3D) paper-based microfluidic chips based on projection-based 3D printing (PBP) technology. A series of two-dimensional (2D) paper-based microfluidic modules was designed and fabricated. After evaluating the effect of exposure time on the accuracy of the flow channel, the resolution of this channel was experimentally analyzed. Furthermore, several 3D paper-based microfluidic chips were assembled based on the 2D ones using different methods, with good channel connectivity. Scaffold-based 2D and hydrogel-based 3D cell culture systems based on 3D paper-based microfluidic chips were verified to be feasible. Furthermore, by combining extrusion 3D bioprinting technology and the proposed 3D paper-based microfluidic chips, multiorgan microfluidic chips were established by directly printing 3D hydrogel structures on 3D paper-based microfluidic chips, confirming that the prepared modular 3D paper-based microfluidic chip is potentially applicable in various biomedical applications.

Mingjun Xie and Zexin Fu have contributed equally to this work.

✉ Yi Sun
13157166766@163.com

✉ Ji Wang
jiwang1004@zju.edu.cn

1 Plastic and Reconstructive Surgery Center, Department of Plastic and Reconstructive Surgery, Zhejiang Provincial People's Hospital, Affiliated People's Hospital, Hangzhou Medical College, Hangzhou 310014, China

2 State Key Laboratory of Fluid Power and Mechatronic Systems, School of Mechanical Engineering, Zhejiang University, Hangzhou 310058, China

3 Key Laboratory of Materials Processing and Mold, Zhengzhou University, Zhengzhou 450002, China

4 Key Laboratory of 3D Printing Process and Equipment of Zhejiang Province, College of Mechanical Engineering, Zhejiang University, Hangzhou 310058, China

5 Cancer Center, Zhejiang University, Hangzhou 310058, China

Graphic abstract

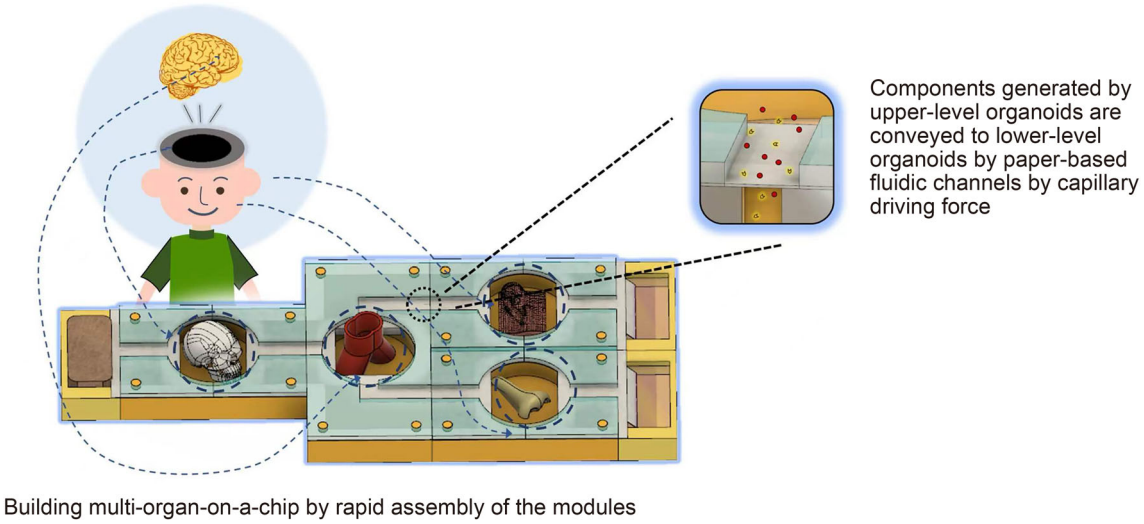

Keywords Paper-based microfluidic chip · Projection-based 3D printing (PBP) · Modularization · Cell culture

Introduction

Developing new drugs requires long-term animal and clinical experiments with several limitations, such as high cost, ethical issues, and strict approval process [1–3]. Moreover, animal experiments cannot simulate the human body, and in vitro experiments using cultured cells do not reflect the effect of drugs on the dynamic physiological environment. Recently, microfluidic systems have become efficient and promising tools in biomedicine because of their significant advantages, such as simulating a dynamic environment, easy control, high visibility, and high integration [4–7]. Therefore, researchers have combined microfluidics with biotechnology to develop a new device called "organ-on-chip," which uses perfused cultured cells to simulate the physiological functions of organs. Research on this "organ-on-chip" system mainly focused on its application in tissue engineering and regenerative medicine. The fabrication of a microfluidic chip, based on a biochip, traditionally involves three steps: (i) fabricating the chip using microfabrication technology, (ii) seeding cells by perfusion, and (iii) culturing cells using pump injection. However, this process has some obvious shortcomings. Creating complex microchannels using traditional manufacturing methods [8–11] and materials [12–14] is difficult. Moreover, because the channel is closed, it is challenging to perfuse cells. Further, multiple cell types and bionic tissue structures cannot be used. Moderate leakage and alignment are unavoidable by injection, and cells or tissues might get damaged due to shear forces. Therefore, a novel fabrication method is urgently needed to overcome these limitations.

The Whitesides group at Harvard University first proposed the concept of paper-based microfluidic chips in 2007 [15]. Since then, paper-based chips have attracted worldwide attention. A paper-based microfluidic chip is a low-cost fluid control device that does not require an external microfluidic device [16]. Its most significant advantage is that it can achieve pumpless drive, and the fluid flows through the capillary driving force of the paper itself. Therefore, creating a specific hydrophobic network on the paper is necessary. Second, the price of filter paper is much lower than that of traditional microfluidic chip substrate materials, such as silicon, and can be used for single use. Moreover, no external device is required, significantly reducing medical testing costs. Paper-based microfluidic chips have many advantages, such as good biocompatibility, simple production, and easy handling. These chips are created by constructing hydrophilic/hydrophobic microstructures or "hydrophobic dams" on paper through a series of processing techniques based on the principle of solidifying hydrophobic materials to restrict the flow of fluids. These dams are usually made of polydimethylsiloxane, SU-8 photoresist, wax, and alkylenone dimer. Recently, manufacturing methods for paper-based microfluidic chips have diversified. Based on the principle of forming a trap dam, these include physical and chemical methods. Physical methods consist of wax printing [17–21], drawing [22, 23], inkjet etching [24, 25], flexo printing [26], laser [27–29], paper cutting [30–35], and

screen printing [36, 37]. Chemical methods include lithography [38], plasma treatment [39], chemical vapor deposition [40], and wet etching [41]. However, all these methods are complex, have high processing costs, and require expensive advanced equipment, which has limited the development of paper-based microfluidic chip technology. For example, although the wax printing method is simple and inexpensive, the microfluidic channel resolution can only be in the millimeter range. In the laser method, the power of the laser and the scanning speed must be carefully selected; otherwise, the parchment gets damaged, invalidating the chip.

Our group has been working on creating organ-on-chips for several years and has found innovative solutions to various problems. In 2015, He et al. proposed a method for manufacturing a microfluidic chip with intricate channels using three-dimensional (3D) printing technology to print sugar as a sacrificial layer [42]. Nie et al. developed a Lego-like modular microfluidic device by 3D printing [43], consisting of various common functional modules, each with a unified standard interface for easy assembly. Due to the open channels in each module, inoculating and handling cells are highly convenient. Furthermore, to overcome issues caused by nutrient solution perfusion, He et al. used filter paper as a substrate to transport fluid through its capillary drive [44]. Accordingly, a simple and low-cost continuous perfusion platform was designed specifically for paper-based microfluidic chips, which was used to establish a dynamic cell culture successfully. Based on these reports, we considered integrating the three ideas by directly printing modular paper-based organ-on-a-chip devices to solve the current problems.

In this paper, we developed a method to fabricate modular 3D paper-based microfluidic chips based on projection-based 3D printing technology (Fig. 1). A series of two-dimensional (2D) paper-based microfluidic modules was designed and fabricated. We also analyzed the effect of exposure time on the accuracy of flow. Based on this analysis, the resolution of the flow channel was experimentally evaluated. Furthermore, using different assembly methods, we assembled several 3D paper-based microfluidic chips based on the 2D ones and obtained good channel connectivity. We designed scaffold-based 2D and hydrogel-based 3D cell culture systems based on these 3D paper-based microfluidic chips, which were verified to be feasible. Furthermore, we created multiorgan microfluidic chips by combining extrusion 3D bioprinting and the prepared 3D paper-based microfluidic chips by directly printing 3D hydrogel structures. This validated the applicability of these modular 3D paper-based microfluidic chips prepared for various biomedical applications.

Materials and methods

Materials and instruments

The projection-based 3D printer was purchased from Shenzhen Nuowa Smart Tech Co. Ltd. (L1121, China). Filter papers and ultraviolet (UV) photosensitive resin were purchased from Whatman Co. Ltd. (Whatman No. 1, UK) and Shenzhen Nuowa Smart Tech Co. Ltd. (Colorless, China), respectively. Food coloring was purchased from Ningbo Weilong Flavors and Fragrances Co. Ltd. (Red, China). The low-speed centrifuge was procured from Hunan Xiangyi Co. Ltd. (TDZ5-WS, China). The constant temperature CO_2 incubator was from STIK Co. Ltd. (IL-161CT, USA). Human umbilical vein endothelial cells (HUVECs) were obtained from the Department of Cardiology of the Second Affiliated Hospital of Zhejiang University School of Medicine, China. Endothelial cell medium (ECM) and phosphate-buffered saline (PBS) were purchased from Sciencell Co. Ltd. (USA) and Hyclone Co. Ltd. (USA), respectively. Gelatin methacryloyl (GelMA) and lithium phenyl-2, 4, 6-trimethylbenzoylphosphinate (LAP) photoinitiator were purchased from Suzhou Intelligent Manufacturing Research Institute (EFL-GM-60, China). Tyrisin was purchased from Gibco Co. Ltd. (1X, USA). Deionized water was purchased from Diena Co., Ltd. (China).

Projection-based 3D printing (PBP) of the 2D paper-based microfluidic module

The microfluidic module model was built using SolidWorks. The thickness of this module was set to 0.3 mm. The STL file was imported into the slicing software Creation Workshop. Detailed layering parameters were set, including slice thickness, exposure time of individual and bottom layers, and rising distance after each exposure. After adding adequate photosensitive resin to the printer's resin tank, the filter paper was placed flat until completely immersed in the resin. The bottom-most structure was printed first. To ensure that the bottom layer firmly adheres to the printing platform and easily separates from the release film, the exposure time of the bottom layers was increased. The bottom layer of resin was cured with the filter paper, and the next layer was cured as the platform rose. The paper-based microfluidic chip was printed after the layers were superimposed. After printing, the printing platform automatically rises, allowing the paper chip to sit for half a minute and the residual resin to remain naturally. After detaching the printing platform , it was washed with

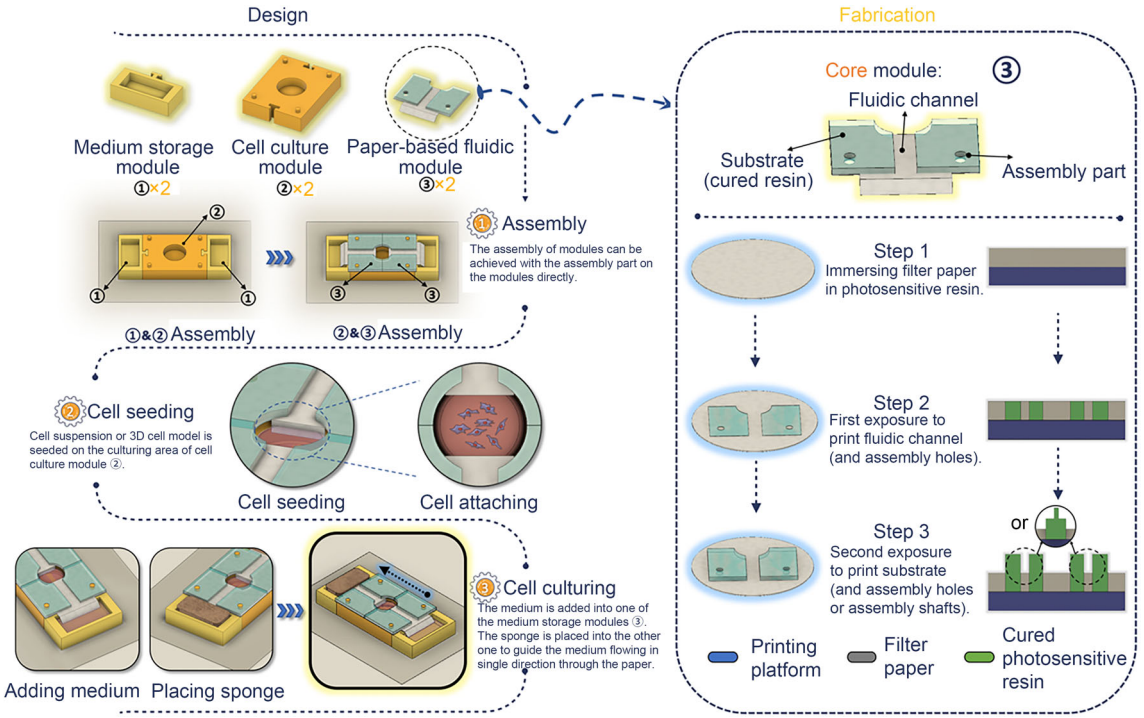

Fig. 1 Schematic of modular 3D paper-based microfluidic chip fabrication using projection-based 3D printing

alcohol along with the printed module to remove the UV photosensitive resin on the surface and in the channel. The 2D paper-based microfluidic module was slowly scraped with a utility knife and air-dried at room temperature. Subsequently, the excess paper was cut along the outline of the module with scissors. In the printing analysis experiment, the flow channel width was 1 mm, and the exposure time was the independent variable. Twenty experimental groups were performed from 31 to 50 s with a time gradient of 1 s. The pigment solution at one end of the flow channel and the width of the channel was observed under an optical microscope and measured.

Dynamic resolution analysis of 2D paper-based microfluidic module

Dynamic resolution refers to the minimum width of a hydrophilic flow channel or a dam through which the fluid can completely flow under the capillary driving force or be blocked entirely, respectively. While both the hydrophilic channel and dam models are characterized by a width gradient of 100 μm, the width of the former from right to left is 100 to 1300 μm, while that of the latter is 300 to 1500 μm. A sufficient amount of pigment solution was dropped into the triangular area. After the solution diffuses and dries, the microstructure of the flow channel is observed under an optical microscope. The smallest hydrophilic channel through which the solution can completely flow and the finest hydrophobic dam through which the solution can be completely blocked are measured.

Concentration gradient test on 2D paper-based microfluidic module

For the concentration gradient test, a 2D paper-based microfluidic module containing two inlets and three outlets was designed. The length × width × thickness of the module is 50 mm × 50 mm × 0.34 mm, and the channel width is 3 mm. Inlet 1 was immersed in the pigment solution through filter paper, while inlet 2 was immersed in deionized water. The two fluids flow and mix under the capillary action of the filter paper, and liquids of different concentrations flow out of the three outlets. As the paper-based microfluidic modules have the advantage of a low background, they are suitable for colorimetric detection. Therefore, after 4 h, the paper-based microfluidic module was removed, and a digital camera or smartphone captured the results in an environment with a uniform light source. After converting the image into grayscale using image processing software (Photoshop), the grayscale values of the three liquid outlets were recorded.

Module design and connectivity of 3D paper-based microfluidic chip

Four types of multifunctional modules were designed for the 3D paper-based microfluidic chips, including inlet, channel,

function, and other modules without paper. The thickness of the paper-based microfluidic chip modules was set to 2 mm. Moreover, three methods were designed to assemble the 3D paper-based microfluidic chips, including stacking, rotating, and sliding, which can be applied on different occasions. Stacked 3D paper-based microfluidic chips, similar to the traditional ones, are mainly obtained by stacking 2D paper-based microfluidic modules layer by layer. The difference is that the modular assembly of the 2D paper-based microfluidic modules occurred synergistically between its structures, making it detachable and easily replaceable. A "rotating" 3D paper-based microfluidic chip was designed based on the hinge member structure, while the "sliding" ones were derived from traditional sliding microfluidic chips. To ensure a valid connection among parts, we added small, rolled filter paper between the connection locations of the modulus. The connectivity of different assembly methods was tested using pigment solution, which was added to a specific place in the 3D paper-based microfluidic chips. The connectivity quality was checked according to the color distribution in different parts by disassembling the chips after the diffusion experiment.

Scaffold-based 2D cell culture on a 3D paper-based microfluidic chip

HUVECs were seeded on a poly ε-caprolactone (PCL) microfiber scaffold, which was fabricated using near-field direction writing technology. The scaffolds were placed in the wells of a 12-well plate and repeatedly soaked in deionized water three times (5 min each). The scaffolds were then soaked in alcohol for 1 h, treated under UV light, and then washed with PBS thrice (5 min each). After adding ECM into the wells, the scaffolds were laid flat at the bottom of the wells using forceps and then placed in the incubator overnight. The HUVECs were seeded on the treated scaffolds the next day. After 24 h, the cell-laden scaffolds were transferred to the designed 3D paper-based microfluidic chip for further culture. The culture medium was changed every three days. The cell-laden scaffolds were tested on the 1st and 5th days of culture, including cell viability with the Calcein Acetoxymethyl Ester (AM)/Propidium Iodide (PI) kit and cytoskeleton observation with rhodamine-labeled.

Hydrogel-based 3D cell culture on 3D paper-based microfluidic chip

Pure GelMA pre-polymer solution was prepared by dissolving freeze-dried GelMA (0.05 g/mL) and LAP (0.05 g/mL) in PBS. The solution was then sterilized using a 0.22 μm filter and stored at 4 °C. The HUVECs were detached and resuspended in the prepared GelMA bioink at 1×10^6 cells/mL cell density. The cell-laden bioink was added to a 9 mm × 2 mm column mold and crosslinked. The cell-laden GelMA hydrogel was then transferred to the designed 3D paper-based microfluidic chip for further culture. The culture medium was changed every three days. The cell viability and cytoskeletal integrity of the cell-laden GelMA hydrogel were tested on the 1st and 5th days using the Calcein AM/PI kit and rhodamine labeling, respectively.

Establishing the multiorgan microfluidic chip

A special 3D paper-based microfluidic chip with several culturing areas was designed. The chip was placed on an extrusion 3D bioprinter, and the GelMA solution was injected into the imprinter using a syringe. The printing nozzle and receiving platform temperatures were at 26 and 20 °C, respectively. The organ models were built using SolidWorks and sliced with Repetier software to acquire the printing path program. The bioink flow rate and nozzle movement speed were set at 150 μL/min and 120 mm/min, respectively. The 20G cone-shaped nozzle was selected as the printing nozzle. The 3D organ structures were directly printed on different culture areas of the designed 3D paper-based microfluidic chip.

Results and discussion

PBP of 2D paper-based microfluidic module

The shape of the flow channel in the 2D paper-based microfluidic module depends entirely on the image displayed by the UV light source. Compared with traditional lithography used to make paper-based chips, this method greatly reduces the cost of making masks and requires only a computer-generated mask model. To demonstrate that the flow channel has good fluidity, we first established the leaf-shaped paper chip (Figs. 2a1 and 2a2), and the pigment solution was dropped into the flow channel. Figure 2a3 shows the time-shift diagram of the final flow channel. The pigment solution can be seen flowing into the flow channel, demonstrating that the flow channel in the prepared 2D paper-based microfluidic module has good pumpless drivability.

The light-cured molding method described here mainly relies on the penetration of the UV photosensitive resin into the filter paper, which cures into a hydrophobic dam to form the required hydrophilic channel. Therefore, the final curing effect of this resin directly determines the accuracy of the 2D paper-based microfluidic module. Figure 2b shows the microscopic diagram of the channel obtained with exposure time of 10, 31, and 50 s. At the appropriate exposure time (Fig. 2b2), the edge of the runner was neat and in better shape. However, if the exposure time is too short, defects (Fig. 2b1) occur at the edge of the channel due to the diffusion of the

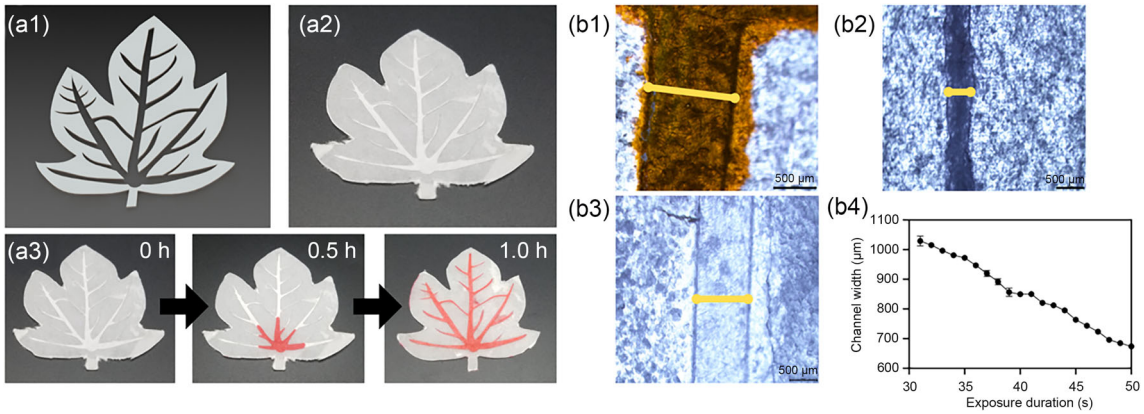

Fig. 2 Projection-based 3D printing (PBP) of 2D paper-based microfluidic module. **a** Leaf-shaped 2D paper-based module fabrication (exposure duration: 31 s): **a1** 3D digital model and **a2** printed module; **a3** pigment solution diffusion in microchannels. **b** Microchannels under different exposure durations: **b1** low exposure duration (10 s); **b2** appropriate exposure duration (31 s); **b3** high exposure duration (50 s); **b4** channel width under different exposure durations

incompletely cured photosensitive resin. This causes a portion of the fluid to seep into the hydrophobic area as the fluid diffuses in the flow channel, creating a leak. If the exposure time is too long, the flow channel becomes distorted, resulting in poor molding. This is probably because the refraction and scattering of light caused by prolonged exposure can cure the resin outside the exposure area. This solidification hinders the smooth formation of the hydrophilic flow channel. The relationship between exposure time and molding accuracy of a 2D paper-based microfluidic module was evaluated. The result (Fig. 2b4) shows that the exposure time and the obtained channel width are negatively correlated. Therefore, we set the optimal exposure time to 33 s. Under this condition, the hydrophilic flow channel of the prepared 2D paper-based microfluidic module has a stable flow rate, uniform flow channel, good molding effect, and is leak-proof.

Dynamic resolution analysis of 2D paper-based microfluidic module

Resolution refers to the minimum width achieved by the hydrophilic channels and traps on a 2D paper-based microfluidic module, which indicates the performance of the paper-based chip. In general, there are two types of resolution: dynamic and static. Dynamic resolution refers to the minimum width of the hydrophilic flow channel or dam through which the fluid can completely flow under the capillary action or can be completely blocked, respectively. Static resolution refers to the minimum width of the hydrophilic flow channel that can be completely immersed in a fluid or a trap dam that will not be immersed in a fluid. For paper-based microfluidic chips, fluids need to flow spontaneously under capillary action. Therefore, the dynamic resolution of paper-based chips is more important. Hence, we mainly investigated the dynamic resolution of 2D paper-based microfluidic modules. The analysis (Figs. 3a and 3b) showed that the fifth channel from left to right is the smallest hydrophilic channel, with a theoretical width of 500 μm. The actual width measured under the optical microscope is (477 ± 3) μm. Similarly, the finest trap dam is the third channel from right to left, with a theoretical width of 500 μm and actual width of (522 ± 3) μm, as measured using optical microscopy.

Concentration gradient test on 2D paper-based microfluidic module

Figures 3c1–3c3 show the 2D paper-based microfluidic module and its color after 4 h of flow. The colors of the outlets in the flow channel were as follows: outlet 3 was white with colorless liquid; outlet 1 was red and dark; outlet 2 was red and the color of the liquid was between that in outlets 1 and 3. This indicates that the liquid in outlet 2 is the product of mixing two liquids, which is consistent with our expectations. Furthermore, we used a smartphone to take an image of the liquid outlet under uniform light conditions and then used Photoshop software to convert the captured image to read the gray values of the three liquid outlets (Fig. 3c4). The concentration of the solution in outlet 2 is approximately half of that in outlets 1 and 3, forming a clear concentration gradient. Notably, the depth of channels will also control the flow of the solution. However, herein, we mainly displayed this method with a controllable 3D topology and function of the modular 3D microfluidic chip. Thus, we only validated the flow rather than the flow rate. Furthermore, in terms of 3D culture, the depth of the channel is mainly determined by the height of the cultured sample rather than the flow rate. Considering these, we did not explore the effect of channel depth on the flow.

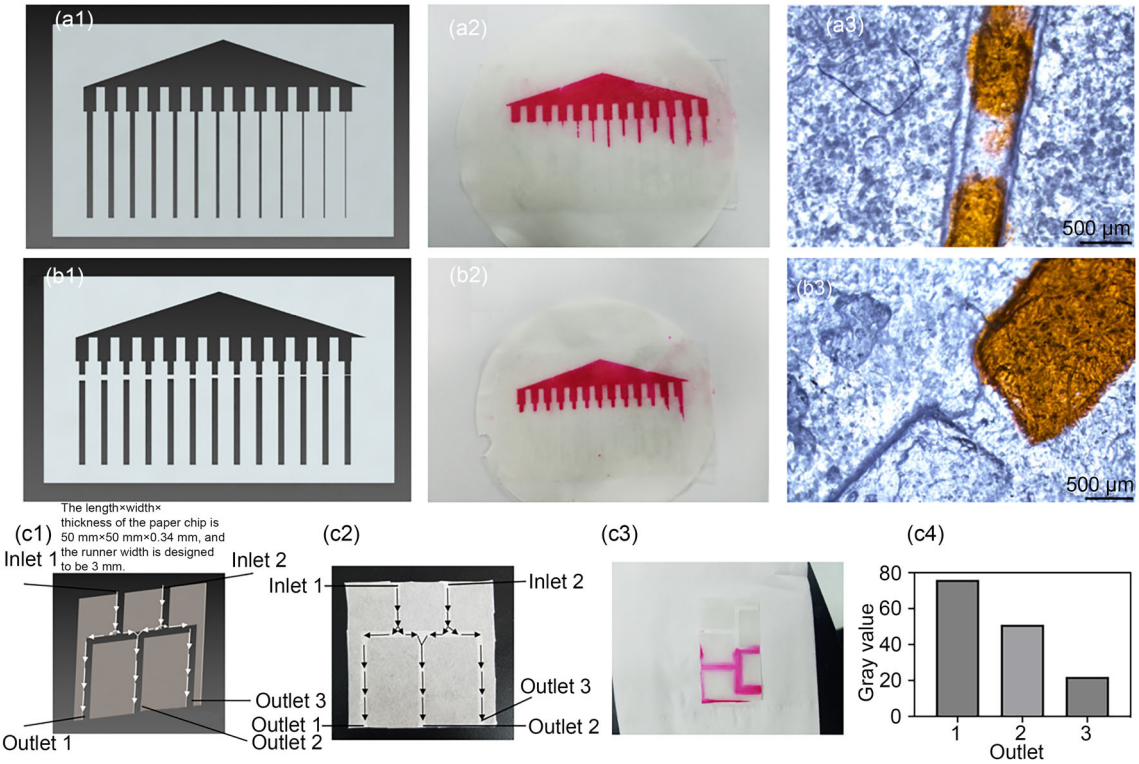

Fig. 3 Channel testing of 2D paper-based module. Dynamic resolution analysis of the (1) digital model, (2) paper-based module, and (3) optical image of the channel of **a** the hydrophobic flow channel and **b** the dam. **c** Concentration gradient test: **c1** digital model of the testing chip; **c2** testing chip before diffusion of pigment solution; **c3** testing chip after pigment solution diffusion; **c4** grayscale values of three outlets after testing

Module design and connectivity of 3D paper-based microfluidic chip

To achieve multistep-ordered chemical reactions or multiple pre-processing steps on a single chip and improve the efficiency of the analytical process, different manufacturing methods are being increasingly researched for 3D paper-based microfluidic chips. Due to its 3D channel network, the 3D paper-based microfluidic chips are more advantageous than the 2D ones. Moreover, compared with 2D paper-based microfluidic chips, the 3D ones have higher flow rates because the length in the z direction is shorter than that in the x–y plane. Further, the 3D paper-based microfluidic chip can be used to conduct several experiments simultaneously, and each layer of this chip can achieve different functions. Therefore, the 3D paper-based microfluidic chip is more capable of meeting the experimental requirements.

In this work, the module design for 3D paper-based microfluidic chips included two factors: functions and assembly. Considering organ chip requirements, such as culture medium supply, medium (with or without cell products or drugs) delivery and interactions, and cell sample culture, the module functions included four categories, namely inlet, channel, and function modules, and another module without paper (Fig. 4). The inlet module is at the beginning of the microfluidic chips. The channel module has a different routine for fluid transportation in different directions, while the function module is applied for different interactions or parameters controlling the chip. Another module without paper is used for cell sample culturing and a container for holding media or waste. Notably, in real-time applications, the overall outline of modules can be modified according to specific requirements as long as the characteristic structures remain.

Regarding module assembly, the assembly holes or bosses are directly printed on different modules using three methods set on the multifunctional module: stack, rotate, and slide assemblies (Fig. 5a).

Stack assembly

Stacked 3D paper-based microfluidic chips resemble the traditional ones and are mainly obtained by stacking paper-based microfluidic modules layer by layer. The difference is that the modular assembly is completed through cooperation

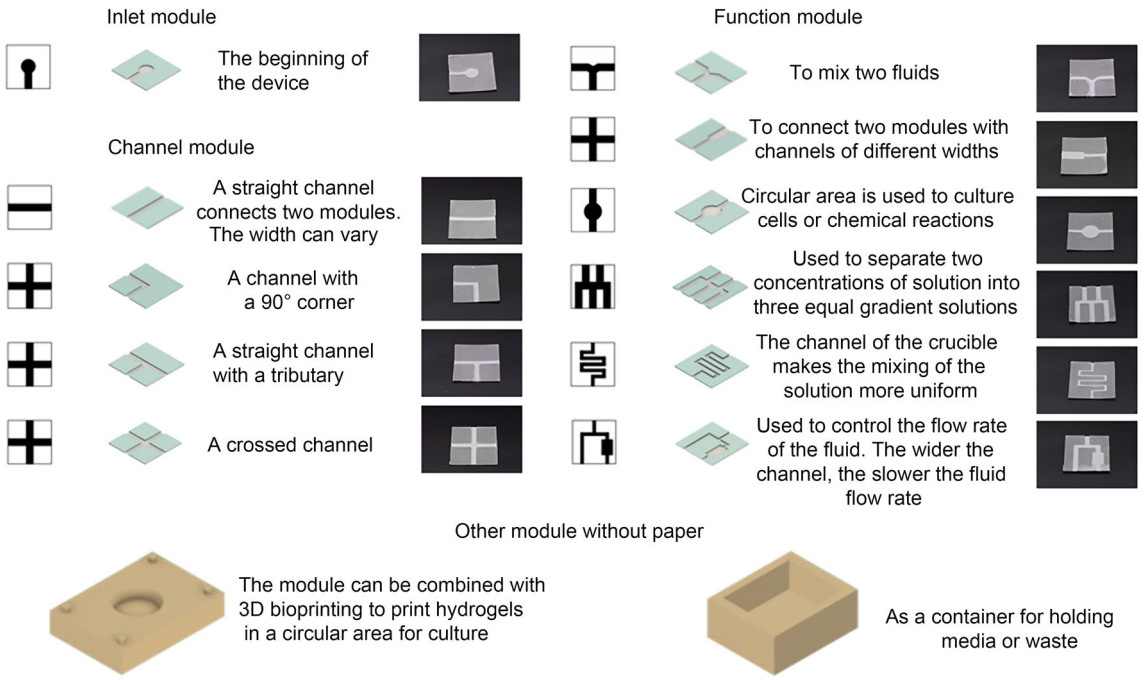

Fig. 4 Multifunctional module design for 3D paper-based microfluidic chips

between its structures, imparting it with the added advantages of detachability and easy replacement. The relatively simple 3D structure of this module includes a narrow groove at the interface of the two modules, which can be inserted into a sliced filter paper to connect the flow channel area of the two 2D paper-based microfluidic chip modules. Using filter paper as the material at the junction provides a stable flow rate, which can be controlled by changing the shape of the filter paper at the junction.

Rotate assembly

The rotated 3D paper-based microfluidic chip is designed according to the hinge member structure. The assembly and rotation of the upper and lower module layers rely on the cooperation of cylindrical bosses and annular grooves. The center of rotation is the connection between the upper and lower layers of the modules, so the flow of fluid is not affected during the rotation. The 3D paper-based microfluidic chip can achieve multilayer superposition, and the rotation of the two connected paper chip modules does not affect the rest of the modules. In practice, the connection can be filled with cellulose powder or filter paper fiber to connect the upper and lower layers of paper chip modules.

Slide assembly

The slide 3D paper-based microfluidic chips, based on traditional sliding microfluidic chips, are suitable for multiplexed liquid phase experiments, which can reduce labor costs and improve efficiency. The two square bosses in the middle of one module can be matched with the square groove track in another module to act as a guide. This prevents slippage when the upper and lower layers of the paper chip module interface coincide. The two modules fit closely by the boss and groove track, and the boss can slide smoothly in the groove track. In practical applications, cellulose powder or filter paper fibers can be filled at the connection to connect the upper and lower layers of modules.

Diffusion tests of these three assembly methods revealed that the pigment solution can flow smoothly through the 3D paper-based microfluidic chip interface. In the stack (Fig. 5b) and rotate (Fig. 5c) assembly methods, under the capillary action of the filter paper, the pigment solution successfully passes through the filter paper at the interface and flows from the upper module to the lower module. In the slide assembly method (Fig. 5d), the pigment solution flows smoothly through the 3D paper-based microfluidic chip interface, with smooth sliding and a tight fit between the modules. This microfluidic chip can artificially control the channel that needs to react and can also be used as a delay device, providing novel ideas for developing 3D paper-based microfluidic chips, such as multichannel reactions.

To further verify the feasibility of the modular 3D paper-based microfluidic chip, we designed a complex chip simultaneously using the stack, rotate, and slide assembly methods (Fig. 5e). Blue and red pigment solutions were added to the two upper modules, separately. The results showed that these

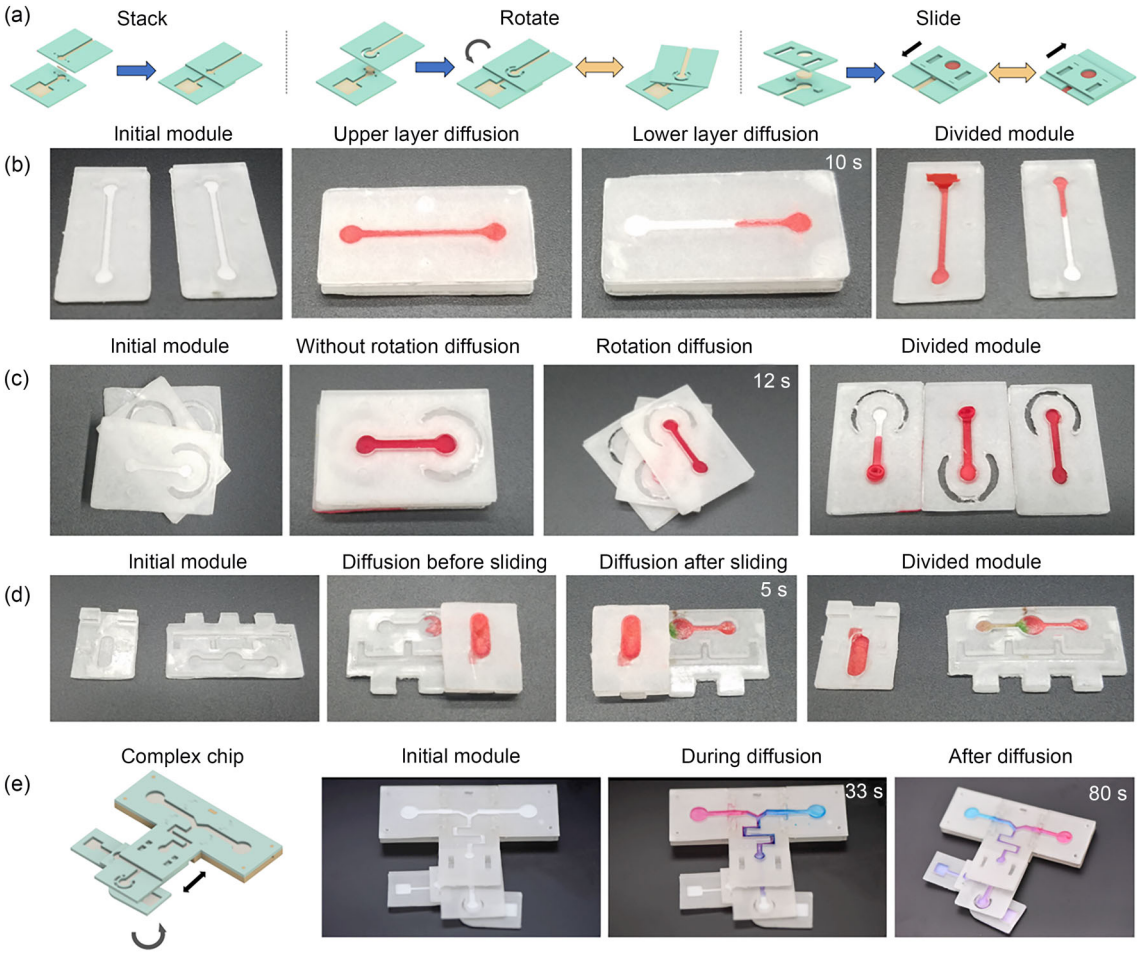

Fig. 5 Assembly methods and diffusion testing of 3D paper-based microfluidic chips. **a** Different assembly methods. Diffusion test of 3D paper-based microfluidic chips based on the **b** stack, **c** rotate, and **d** slide assembly methods. **e** A complex chip made using stack, rotate, and slide assembly methods and its diffusion test

solutions gradually mixed and diffused toward the lower layers. Finally, the mixed pigment solution successfully reached the lowest layer, verifying the feasibility of the proposed modular strategy to establish an on-demand complex 3D paper-based microfluidic chip.

In the actual assembly, we included a small, rolled filter paper between the connection of the modulus to ensure a valid flow connection. Thus, the flow was derived from the normal capillary effect rather than liquid wicking, which can be described by the Lucas–Washburn equation. However, modular 3D microfluidic chips can be developed in the future based on the Lucas–Washburn equation for easier assembly without using rolled filter paper.

Scaffold-based 2D cell culture on 3D paper-based microfluidic chip

Tissue engineering scaffolds are widely applied in biomedicine research [45]. A special modular chip was assembled to test the cell culturing capability of the proposed method (Fig. 6a). The cell sample can be placed in the middle rut of the chip as the culture area. One container is loaded with fresh nutrient medium for the cells, and the other one is loaded with a sponge to drive the medium's flow and collect waste. A HUVEC-laden PCL scaffold is placed in the culture area (Fig. 6b). The viability of the HUVECs on the PCL scaffold was tested with the live/dead reagent on the 1st and 5th days of culturing, which showed that most cells remained in the live state on the scaffold (Fig. 6c). Moreover, the cytoskeletal morphology images (Fig. 6d) revealed that, on the first day of culture, HUVECs successfully attached to the scaffold surface, and on the fifth day, the cells formed

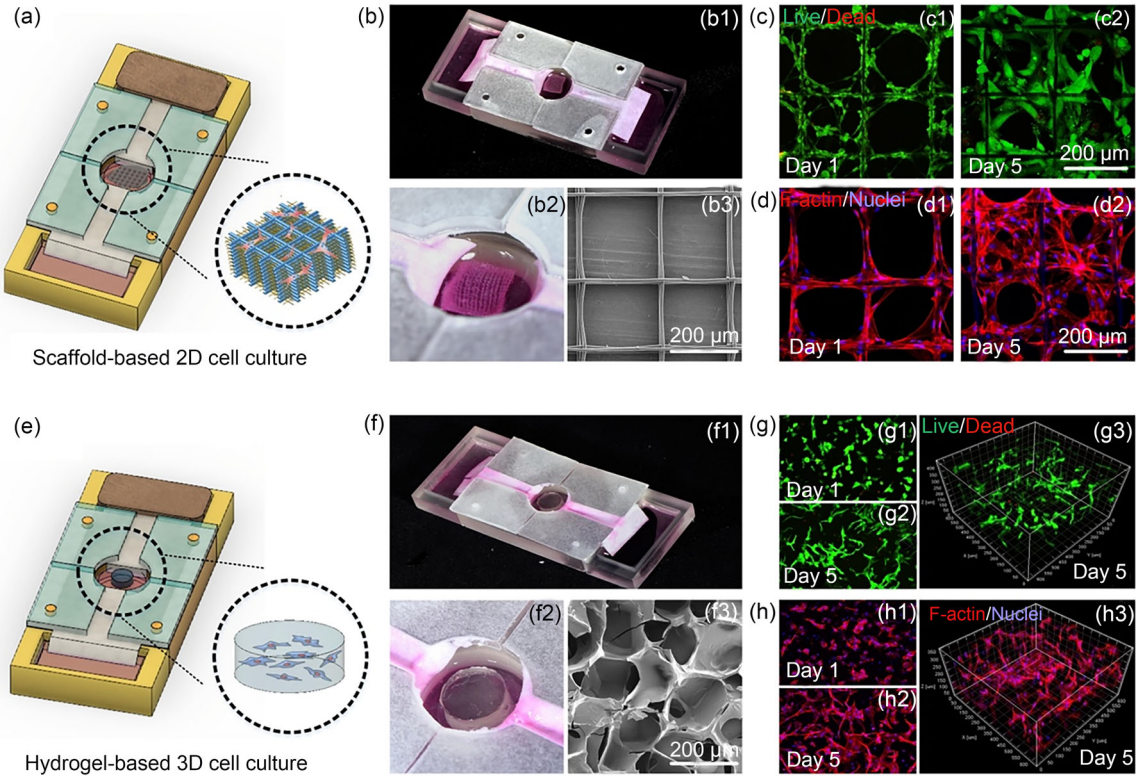

Fig. 6 2D and 3D cell culture on 3D paper-based microfluidic chips. **a** Scaffold-based 2D cell culture sketch. **b** Photos of 3D paper-based microfluidic chips with a scaffold-based 2D cell sample. **c** Live/dead testing of human umbilical vein endothelial cells (HUVECs) on the poly ε-caprolactone (PCL) scaffolds. **d** Morphology of HUVECs on the PCL scaffolds stained by phalloidin and 4',6-diamidino-2-phenylindole (DAPI). **e** Hydrogel-based 3D cell culture sketch. **f** Photos of 3D paper-based microfluidic chips with a hydrogel-based 3D cell sample. **g** Live/dead testing of HUVECs in the gelatin methacryloyl (GelMA) hydrogel. **h** Morphology of HUVECs in the GelMA hydrogel stained by phalloidin and DAPI

dense cell groups on the scaffold. These results indicate that 2D cell culture on the 3D paper-based microfluidic chip can maintain cellular activity and function.

Hydrogel-based 3D cell culture on 3D paper-based microfluidic chip

The physicochemical properties of the hydrogel, widely used in bio-fabrication, can induce cell functionalization [46]. The HUVEC-laden GelMA hydrogel was placed in the culture area (Figs. 6e and 6f) of the same chip for the scaffold-based 2D cell culture test. The viability of the HUVECs in the GelMA hydrogel was tested with the live/dead reagent on the 1st and 5th day of culture, which showed that most cells remained alive (Fig. 6g). Based on the cytoskeleton morphology images (Fig. 6h), on the 1st day of culture, the HUVECs started to spread in the 3D microenvironment until the 5th day. These results indicate that 3D cell culture on a 3D paper-based microfluidic chip can maintain cellular activity and function.

The results of the 2D and 3D culture on the 3D paper-based microfluidic chips show that, compared to the traditional culturing systems like Petri dishes, the cell samples have a continuous supply of fresh culture medium. Although this might maintain sterility during culture, the antibacterial capability of paper is probably lower than that of plastics.

Establishing a multiorgan microfluidic chip

Multiorgan microfluidic chips have significant biomedical implications because they can simulate complex interactions among different cells/tissues/organs. Here, we combined microfluidic chips and 3D bioprinting technologies [47, 48] to establish multiorgan microfluidic chips with different 3D organ samples directly. A special 3D paper-based microfluidic chip with several culturing areas (Fig. 7a) was designed. The chip was placed on an extrusion 3D imprinter. Four 3D organ structures, namely the skull, nose, ear, and vessel, were built and printed using an extrusion 3D imprinter and the GelMA bioink. The results showed that the four GelMA-based organ structures can be successfully built on

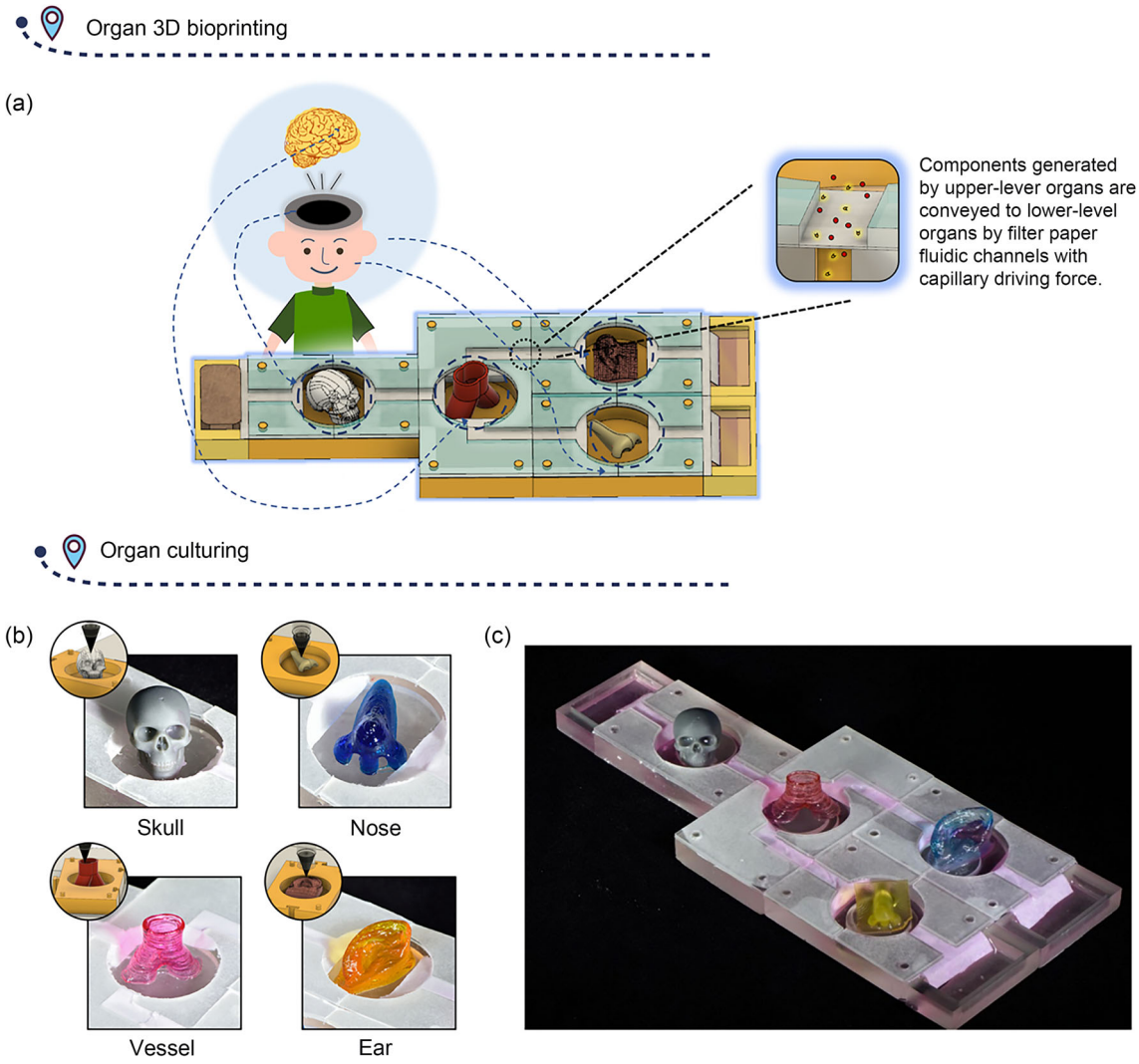

Fig. 7 Establishment of the multiorgan microfluidic chip. **a** Schematic diagram of the multiorgan microfluidic chip. Photos of **b** the 3D organ structure directly printed on the chip and **c** the chip itself

the culture area of the 3D paper-based microfluidic chips (Fig. 7b). Consequently, by combining 3D GelMA-based organ structures and the 3D paper-based microfluidic chip, a multiorgan microfluidic chip was successfully established (Fig. 7c), showing the potential applicability of the proposed modular assembly strategy in biomedicine.

Conclusions

This study uses PBP technology to prepare 3D paper-based microfluidic chips successfully. This method has several advantages, including easy operation, low cost, high precision, and good applicability for mass production. More importantly, based on the characteristics of PBP, we creatively modularized 3D paper-based microfluidic chips, which can be easily assembled by their own structure, providing the added advantages of easy disassembly and replacement. The channel flow and cell experimental results are good, which confirms that the 3D paper-based microfluidic chips obtained by the PBP method have good feasibility and biocompatibility. These methods can be used to develop novel biomedical applications in the future.

Acknowledgements This study was sponsored by the National Natural Science Foundation of China (No. 52235007, YH), the Science Fund for Creative Research Groups of the National Natural Science Foundation of China (No. T2121004, YH), the National Natural Science Foundation of China (No. 52305300, MJX), the Fellowship of China Postdoctoral Science Foundation (No. 2022M722826, MJX), the National Natural Science Foundation of China (No. 82203602, JW), and the Zhejiang Provincial Natural Science Foundation of China (No. LQ22H160020, JW).

Author contributions Conceptualization was contributed by YH, MJX, CFL; investigation was contributed by YS, JW, LP; methods and experiments were contributed by CFL, MJX; writing—original draft, was

contributed by MJX, ZXF; writing—review and editing, was contributed by YH, SFW, JW.

Declarations

Conflict of interest YH is an associate editor for *Bio-Design and Manufacturing* and was not involved in the editorial review or the decision to publish this article. The authors declare that they have no conflict of interest.

Ethical approval This article does not contain any studies with human or animal subjects performed by any of the authors.

References

1. Eglen RM, Randle DH (2015) Drug discovery goes three-dimensional: goodbye to flat high-throughput screening? ASSAY Drug Dev Technol 13(5):262–265. https://doi.org/10.1089/adt.2015.647
2. Santo VE, Rebelo SP, Estrada MF et al (2017) Drug screening in 3D in vitro tumor models: overcoming current pitfalls of efficacy readouts. Biotechnol J 12(1):1600505. https://doi.org/10.1002/biot.201600505
3. Xie MJ, Gao Q, Fu JZ et al (2020) Bioprinting of novel 3D tumor array chip for drug screening. Bio-Des Manuf 3(3):175–188. https://doi.org/10.1007/s42242-020-00078-4
4. Whitesides GM (2006) The origins and the future of microfluidics. Nature 442(7010):368–373. https://doi.org/10.1038/nature05058
5. Ren KN, Zhou JH, Wu HK (2013) Materials for microfluidic chip fabrication. Acc Chem Res 46(11):2396–2406. https://doi.org/10.1021/ar300314s
6. Shrimal P, Jadeja G, Patel S (2020) A review on novel methodologies for drug nanoparticle preparation: microfluidic approach. Chem Eng Res Des 153:728–756. https://doi.org/10.1016/j.cherd.2019.11.031
7. Hamdallah SI, Zoqlam R, Erfle P et al (2020) Microfluidics for pharmaceutical nanoparticle fabrication: the truth and the myth. Int J Pharm 584:119408. https://doi.org/10.1016/j.ijpharm.2020.119408
8. Convery N, Gadegaard N (2019) 30 years of microfluidics. Micro Nano Eng 2:76–91. https://doi.org/10.1016/j.mne.2019.01.003
9. Hunt M, Taverne M, Askey J et al (2020) Harnessing multi-photon absorption to produce three-dimensional magnetic structures at the nanoscale. Materials 13(3):761. https://doi.org/10.3390/ma13030761
10. Gale BK, Jafek AR, Lambert CJ et al (2018) A review of current methods in microfluidic device fabrication and future commercialization prospects. Inventions 3(3):60. https://doi.org/10.3390/inventions3030060
11. Gross BC, Erkal JL, Lockwood SY et al (2014) Evaluation of 3D printing and its potential impact on biotechnology and the chemical sciences. Anal Chem 86(7):3240–3253. https://doi.org/10.1021/ac403397r
12. Singh A, Malek CK, Kulkarni SK (2010) Development in microreactor technology for nanoparticle synthesis. Int J Nanosci 9(2):93–112
13. Martins JP, Torrieri G, Santos HA (2018) The importance of microfluidics for the preparation of nanoparticles as advanced drug delivery systems. Expert Opin Drug Deliv 15(5):469–479. https://doi.org/10.1080/17425247.2018.1446936
14. Campbell SB, Wu QH, Yazbeck J (2021) Beyond polydimethylsiloxane: alternative materials for fabrication of organ-on-a-chip devices and microphysiological systems. ACS Biomater Sci Eng 7(7):2880–2899. https://doi.org/10.1021/acsbiomaterials.0c00640
15. Martinez AW, Phillips ST, Butte MJ et al (2007) Patterned paper as a platform for inexpensive, low-volume, portable bioassays. Angew Chem 46(8):1318–1320. https://doi.org/10.1002/anie.200603817
16. Li HB, Cheng F, Robledo-Lara JA et al (2020) Fabrication of paper-based devices for in vitro tissue modeling. Bio-Des Manuf 3(3):252–265. https://doi.org/10.1007/s42242-020-00077-5
17. Lu Y, Shi WW, Jiang L et al (2009) Rapid prototyping of paper-based microfluidics with wax for low-cost, portable bioassay. Electrophoresis 30(9):1497–1500. https://doi.org/10.1002/elps.200800563
18. Carrilho E, Martinez AW, Whitesides GM (2009) Understanding wax printing: a simple micropatterning process for paper-based microfluidics. Anal Chem 81(16):7091–7095. https://doi.org/10.1021/ac901071p
19. Schilling KM, Lepore AL, Kurian JA et al (2012) Fully enclosed microfluidic paper-based analytical devices. Anal Chem 84(3):1579–1585. https://doi.org/10.1021/ac202837s
20. Songjaroen T, Dungchai W, Chailapakul O et al (2011) Novel, simple and low-cost alternative method for fabrication of paper-based microfluidics by wax dipping. Talanta 85(5):2587–2593. https://doi.org/10.1016/j.talanta.2011.08.024
21. Zhang AL, Zha Y (2012) Fabrication of paper-based microfluidic device using printed circuit technology. AIP Adv 2(2):022171. https://doi.org/10.1063/1.4733346
22. Bruzewicz DA, Reches M, Whitesides GM (2008) Low-cost printing of poly(dimethylsiloxane) barriers to define microchannels in paper. Anal Chem 80(9):3387–3392. https://doi.org/10.1021/ac702605a
23. Nie JF, Zhang Y, Lin LW et al (2012) Low-cost fabrication of paper-based microfluidic devices by one-step plotting. Anal Chem 84(15):6331–6335. https://doi.org/10.1021/ac203496c
24. Abe K, Suzuki K, Citterio D (2008) Inkjet-printed microfluidic multianalyte chemical sensing paper. Anal Chem 80(18):6928–6934. https://doi.org/10.1021/ac800604v
25. Abe K, Kotera K, Suzuki K et al (2010) Inkjet-printed paperfluidic immuno-chemical sensing device. Anal Bioanal Chem 398(2):885–893. https://doi.org/10.1007/s00216-010-4011-2
26. Olkkonen J, Lehtinen K, Erho T (2010) Flexographically printed fluidic structures in paper. Anal Chem 82(24):10246–10250. https://doi.org/10.1021/ac1027066
27. Chitnis G, Ding ZW, Chang CL et al (2011) Laser-treated hydrophobic paper: an inexpensive microfluidic platform. Lab Chip 11(6):1161–1165. https://doi.org/10.1039/c0lc00512f
28. Spicar-Mihalic P, Toley B, Houghtaling J et al (2013) CO_2 laser cutting and ablative etching for the fabrication of paper-based devices. J Micromech Microeng 23(6):067003. https://doi.org/10.1088/0960-1317/23/6/067003
29. Nie JF, Liang YZ, Zhang Y et al (2013) One-step patterning of hollow microstructures in paper by laser cutting to create microfluidic analytical devices. Analyst 138(2):671–676. https://doi.org/10.1039/c2an36219h
30. Fenton EM, Mascarenas MR, López GP et al (2009) Multiplex lateral-flow test strips fabricated by two-dimensional shaping. ACS Appl Mater Interface 1(1):124–129. https://doi.org/10.1021/am800043z
31. Cassano CL, Fan ZH (2013) Laminated paper-based analytical devices (LPAD): fabrication, characterization, and assays. Microfluid Nanofluid 15(2):173–181. https://doi.org/10.1007/s10404-013-1140-x
32. Giokas DL, Tsogas GZ, Vlessidis AG (2014) Programming fluid transport in paper-based microfluidic devices using razor-crafted open channels. Anal Chem 86(13):6202–6207. https://doi.org/10.1021/ac501273v

33. Glavan AC, Martinez RV, Maxwell EJ et al (2013) Rapid fabrication of pressure-driven open-channel microfluidic devices in omniphobic RF paper. Lab Chip 13(15):2922–2930. https://doi.org/10.1039/c3lc50371b
34. Renault C, Li X, Fosdick SE et al (2013) Hollow-channel paper analytical devices. Anal Chem 85(16):7976–7979. https://doi.org/10.1021/ac401786h
35. Thuo MM, Martinez RV, Lan WJ et al (2014) Fabrication of low-cost paper-based microfluidic devices by embossing or cut-and-stack methods. Chem Mater 26(14):4230–4237. https://doi.org/10.1021/cm501596s
36. Dungchai W, Chailapakul O, Henry CS (2011) A low-cost, simple, and rapid fabrication method for paper-based microfluidics using wax screen-printing. Analyst 136(1):77–82. https://doi.org/10.1039/c0an00406e
37. Sameenoi Y, Nongkai PN, Nouanthavong S et al (2014) One-step polymer screen-printing for microfluidic paper-based analytical device (μPAD) fabrication. Analyst 139(24):6580–6588. https://doi.org/10.1039/c4an01624f
38. Aazmi A, Guo ZX, Yu HR et al (2023) Enhanced mixing efficiency for a novel 3D Tesla micromixer for Newtonian and non-Newtonian fluids. J Zhejiang Univ-SCI A (Appl Phys & Eng) 24(12):1065–1078. https://doi.org/10.1631/jzus.A2300589
39. Zhao DK, Xu HQ, Yin J et al (2022) Inkjet 3D bioprinting for tissue engineering and pharmaceutics. J Zhejiang Univ-SCI A (Appl Phys & Eng) 23(12):955–973. https://doi.org/10.1631/2023.A2200569
40. Kwong P, Gupta M (2012) Vapor phase deposition of functional polymers onto paper-based microfluidic devices for advanced unit operations. Anal Chem 84(22):10129–10135. https://doi.org/10.1021/ac302861v
41. Cai LF, Xu CX, Lin SH et al (2014) A simple paper-based sensor fabricated by selective wet etching of silanized filter paper using a paper mask. Biomicrofluidics 8(5):056504. https://doi.org/10.1063/1.4898096
42. He Y, Qiu JJ, Fu JZ et al (2015) Printing 3D microfluidic chips with a 3D sugar printer. Microfluid Nanofluid 19:447–456. https://doi.org/10.1007/s10404-015-1571-7
43. Nie J, Gao Q, Qiu JJ et al (2018) 3D printed Lego®–like modular microfluidic devices based on capillary driving. Biofabrication 10(3):035001. https://doi.org/10.1088/1758-5090/aaadd3
44. He Y, Wu Y, Fu JZ et al (2016) Developments of 3D printing microfluidics and applications in chemistry and biology: a review. Electroanalysis 28(8):1658–1678. https://doi.org/10.1002/elan.201600043
45. Lu Y, Li G, Li YQ et al (2023) Cellulose nanofibril matrix drives the dynamic formation of spheroids. J Zhejiang Univ-SCI B (Biomed & Biotechnol) 24(10):922–934. https://doi.org/10.1631/jzus.B23d0003
46. Wang ZL, Yang JJ, Sun XH et al (2023) Exosome-mediated regulatory mechanisms in skeletal muscle: a narrative review. J Zhejiang Univ-SCI B (Biomed & Biotechnol) 24(1):1–14. https://doi.org/10.1631/jzus.B2200243
47. Martinez AW, Phillips ST, Butte MJ et al (2007) Patterned paper as a platform for inexpensive, low-volume, portable bioassays. Angew Chem 119(8):1340–1342. https://doi.org/10.1002/ange.200603817
48. Li X, Tian JF, Nguyen T et al (2008) Paper-based microfluidic devices by plasma treatment. Anal Chem 80(23):9131–9134. https://doi.org/10.1021/ac801729t